Electronic Supplementary Material (ESI) for RSC Advances.

Figure S1. Nitrogen adsorption-desorption isotherms for P-25 (A) and Fe_3O_4@TiO_2 (B).

Figure S2. (A) XPS fully scanned spectra for Fe_3O_4; (B) XPS fully scanned spectra and XPS spectra of Ti 2p (inset) for Fe_3O_4@mTiO_2.

Figure S3. Magnetic hysteresis curves of Fe_3O_4, Fe_3O_4@TiO_2, and Fe_3O_4@mTiO_2.

Figure S4. Changes in the concentration of Moncrotophos under the photolysis and Fe_3O_4@mTiO_2 condition with visible light illumination.

Figure S5. (A) Effect of initial concentration on degradation of Moncrotophos; (B) The relationship curves of the ln (C_t/C_0) versus reaction time for different initial concentrations of Moncrotophos. C_t is the Moncrotophos concentration at time t, and C_0 is that in the initial solution.

Figure S6. (A) Effect of pH on degradation of Moncrotophos; (B) The relationship curves of the ln (C_t/C_0) versus reaction time for different initial concentrations of Moncrotophos. C_t is the Moncrotophos concentration at time t, and C_0 is that in the initial solution.

Figure S7. Zeta potential of Fe_3O_4@mTiO_2 nanocomposites and P-25 nanoparticles.

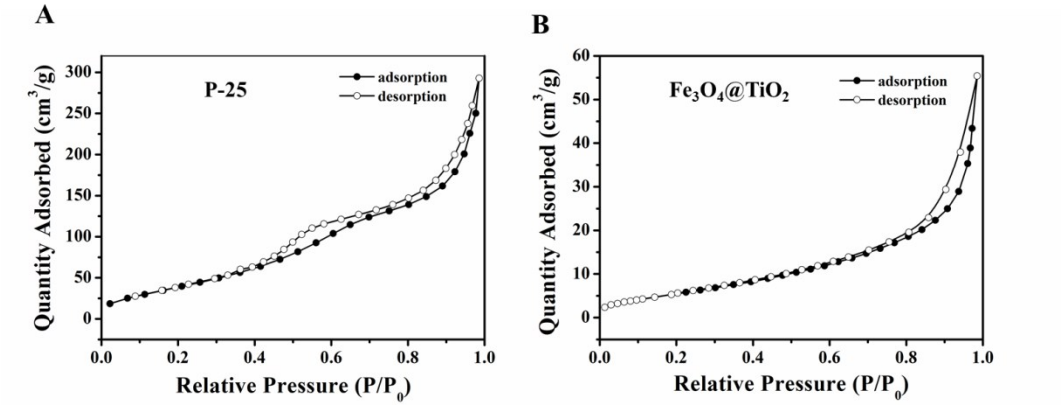

Figure S1.

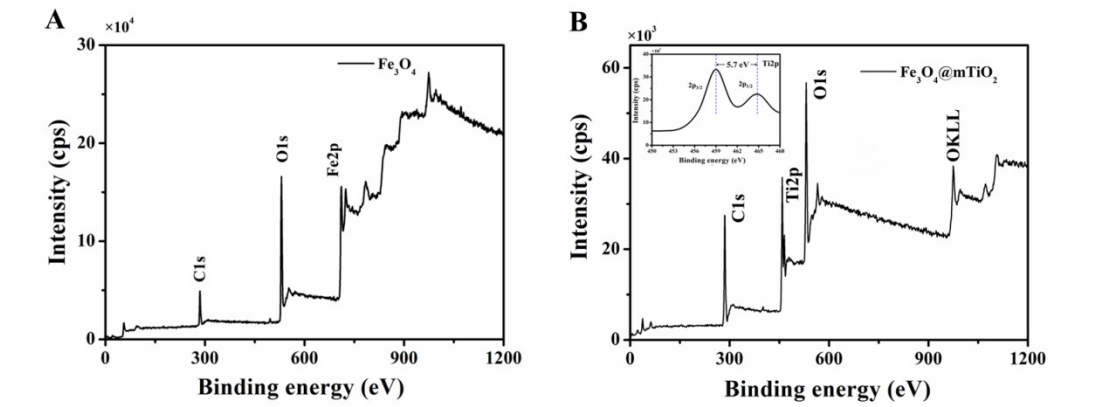

Figure S2.

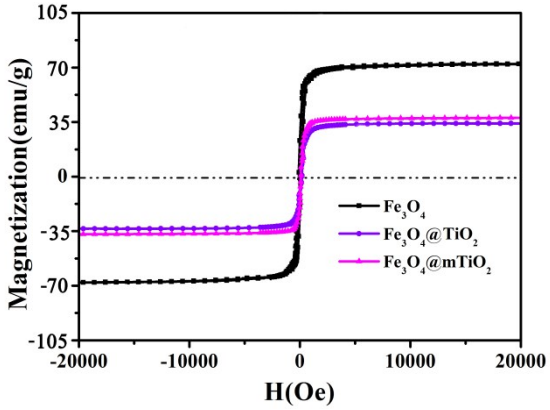

Figure S3.

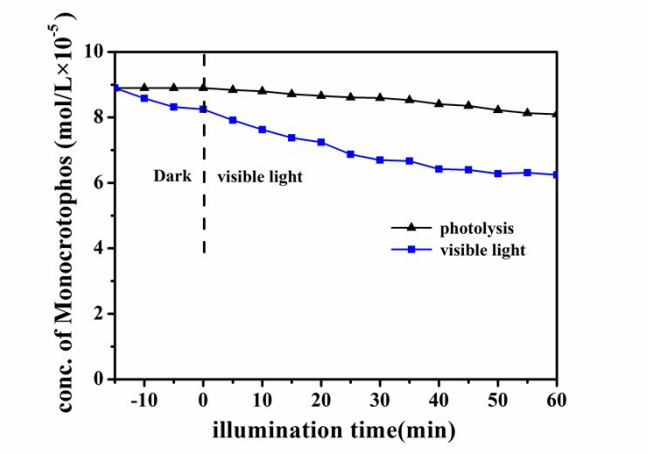

Figure S4.

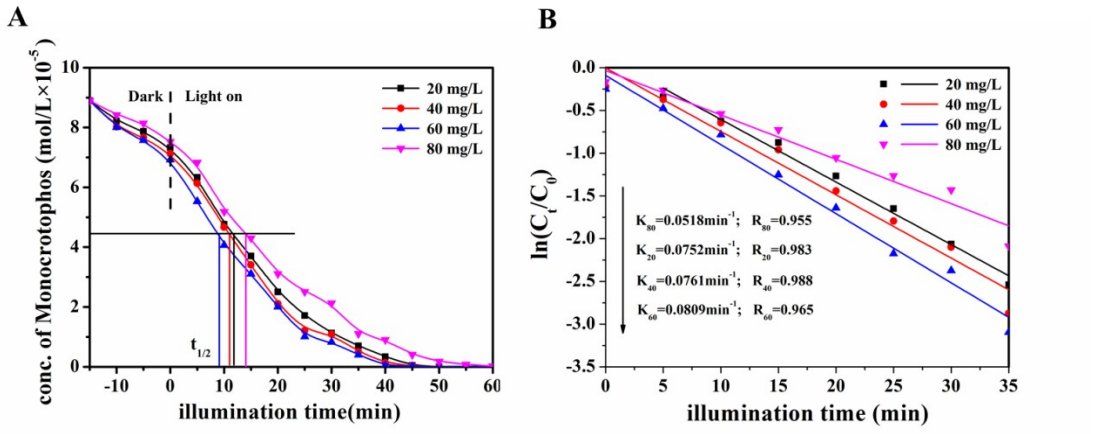

Figure S5.

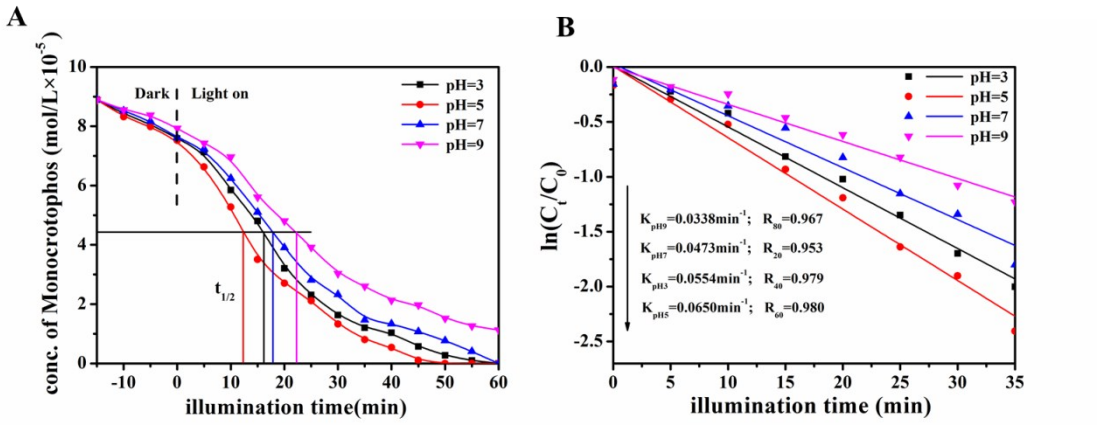

Figure S6.

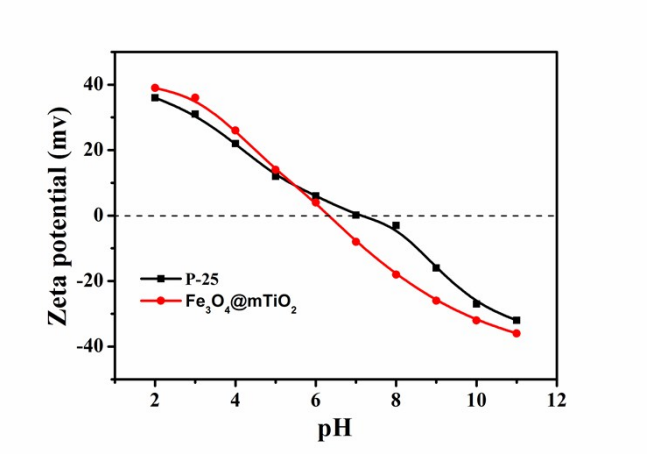

Figure S7.

1. The XPS analysis of Fe_3O_4 and Fe_3O_4@mTiO_2.

XPS analysis was carried out to elucidate the detailed surface chemical composition of synthesized nanoparticles' surface. As shown in Figure S2A, the main peaks of Fe_3O_4 are C 1s, O 1s and Fe 2p centered at 284.9 eV, 530.1 eV and 710.6 eV, respectively. In the Fe_3O_4@mTiO_2 nanocomposites spectrum (Figure S2B), a new peak appears at 459.7 eV, assigned to the photoelectrons originating from the Ti 2p energy level, which responds to the Ti element in the nanocomposites photocatalyst. Compared with Fe_3O_4 spectrum, the signal of Fe 2p decreases and nearly disappears, which is in response to the TiO_2 content in Fe_3O_4@mTiO_2 nanocomposites. Furthermore, the Ti 2p high resolution XPS spectra are showed in Figure S2-B (insert). The two peaks centered at 464.2 and 458.5 eV are well corresponded to Ti $2p_{1/2}$ and Ti $2p_{3/2}$ binding energies. And the splitting energies between them are 5.7 eV, indicating a normal state of Ti^{4+} in the Fe_3O_4@mTiO_2 nanocomposites. These results suggested that Fe_3O_4 and TiO_2 were present mainly as separated phases in the Fe_3O_4@mTiO_2 nanocomposites.

2. The magnetic properties analysis of Fe_3O_4, Fe_3O_4@TiO_2, and Fe_3O_4@mTiO_2.

The magnetic properties of the prepared samples were measured with a VSM. Figure S3 shows the magnetization (M–H) curves of Fe_3O_4, Fe_3O_4@TiO_2, and Fe_3O_4@mTiO_2. It can be seen that saturation magnetization value of Fe_3O_4@TiO_2 (34 emu/g) is much lower than that of the bare Fe_3O_4 (68 emu/g). The decrease in saturation magnetization is mainly due to the non-magnetic titanium dioxide content in the nanocomposites. After mesoporous treatment, the saturation magnetization

value of Fe_3O_4@mTiO_2 (37 emu/g) is little higher than Fe_3O_4@TiO_2 (34 emu/g) because of the mesoporous structure on the surface. Besides, the coercivity (Hc) and remanent magnetization (Mr) of the Fe_3O_4@mTiO_2 nanocomposites are close to zero, indicating that Fe_3O_4@mTiO_2 photocatalyst exhibits superparamagnetic properties at room temperature. With superparamagnetic properties, the magnetic photocatalyst can be recovered efficiently by imparting an external magnetic field and no residual magnetism exists after removal of the applied magnetic field. Therefore, the prepared Fe_3O_4@mTiO_2 photcatalyst can be easily redispersed in solution for recycling.

3. Photocatalytic activity of Moncrotophos in aqueous solution under visible light.

In addition, we also evaluated the photocatalytic activity under visible light because of the Fe_3O_4@mTiO_2 photocatalyst improves the titania response from the UV to the visible region. The experimental conditions are same as the test of photocatalytic activity of Moncrotophos in aqueous solution with Fe_3O_4@mTiO_2 except for visible light. The photocatalytic degradation of Moncrotophos in the presence or in the absence of the Fe_3O_4@mTiO_2 photocatalyst is presented in Figure S4. The result shows that illumination in the absence of Fe_3O_4@mTiO_2 does not result in the distinct photocatalytic degradation of Moncrotophos. And in the presence of Fe_3O_4@mTiO_2, the concentration of Moncrotophos decreases substantially with continued illumination of visible light. While, the photocatalytic efficiency under visible light is much lower than that of UV light. According to Figure S4, we can calculate that about 30% of Moncrotophos can be photo-degradated with 60 min visible light illumination, yet, total of that with UV light. From the result we can

deduce that the Fe_3O_4@mTiO_2 photocatalyst actually improves the titania response from the UV to the visible region.

4. Zeta potential analysis of Fe_3O_4@mTiO_2.

Zeta potential was also analyzed at different pH values in order to study the surface properties of Fe_3O_4@mTiO_2. The zeta potential of nanocomposites in suspensions is probably controlled by the pH through the following process:

$$TiOH_2^+ \underset{+H^+}{\overset{-H^+}{\rightleftharpoons}} TiOH \underset{+H^+}{\overset{-H^+}{\rightleftharpoons}} TiO^-$$

As shown in Figure S7, the zeta potential vs. pH curve for Fe_3O_4@mTiO_2 was similar with that for pure TiO_2 (P-25), suggesting the small influence of the existence of Fe_3O_4 on zeta potential of TiO_2 mesoporous shell. The isoelectric point (IEP) of Fe_3O_4@mTiO_2 and P-25 in deionized water was 6.0 and 7.0, respectively, which is close to the values reported in the literature. The lower IEP of Fe_3O_4@mTiO_2 nanocomposites suggests better dispersions stability around neutral pH, as compared P-25, due to a lager repulsive electrostatic interaction. The difference of zeta potential might be due to the changes in specific surface area and the adsorptive abilities to hydroxyl ions on surface of Fe_3O_4@mTiO_2. Besides, the mesoporous treatment process of the Fe_3O_4@mTiO_2 could alter the surface energy, which results in different adsorption and affinity of protons on the surface. These factors contribute to the minor changes of the zeta potential of Fe_3O_4@mTiO_2.